A New Computer Vision–based System to Help Clinicians Objectively Assess Visual Pursuit with the Moving Mirror Stimulus for the Diagnosis of Minimally Conscious State

Thomas Hoyoux[1]*, Sarah Wannez[2]*, Thomas Langohr[1],
Jérôme Wertz[3], Steven Laureys[2], Jacques G. Verly[1]

[1] Laboratory for Signal and Image Exploitation, University of Liège, Liège, Belgium
[2] Coma Science Group, University of Liège, Liège, Belgium
[3] Phasya S.A., Liège, Belgium

{thomas.hoyoux, sarah.wannez}@ulg.ac.be

Abstract

Minimally conscious state (MCS) is a neurological syndrome in which the patient shows signs of partial consciousness after having emerged from unresponsive wakefulness syndrome (UWS), which itself follows a state of coma. Distinguishing between MCS and UWS is complex and has major impact on the clinical management and prognosis of affected patients. Research on disorders of consciousness (DoC) has revealed that (1) visual pursuit, i.e. the ability of a patient to track a moving stimulus, is one of the most decisive clinical signs for establishing the MCS/UWS distinction, and that (2) the most effective moving stimulus for visual pursuit assessment is a mirror where the patient can see his/her own face. In clinical practice, while this guidance is widely followed, the visual pursuit ability is typically assessed on the basis of the clinician's opinion only, i.e. in a subjective thus biased manner. In this paper, we present a new system using cameras and computer vision techniques, which helps clinicians to objectify the assessment of visual pursuit. Our system is specifically designed to work with the moving mirror stimulus in order to follow the recommended, well-established clinical setup. We validate our system on healthy control subjects and give preliminary results obtained with DoC patients.

1. Introduction

Appropriate clinical management and accurate diagnosis and prognosis of patients with disorders of consciousness (DoC), *e.g.* coma due to a severe brain injury, constitute a complex task that has engaged the efforts of medical doctors and researchers in neuroscience for many decades (going back to the mid-1960s [11]). Coma patients may evolve into so-called unresponsive wakefulness syndrome (UWS, previously called vegetative state) [6], then into so-called minimally conscious state (MCS) [2], where they show behavioral evidence of partial consciousness. The distinction between MCS and UWS can be very challenging to make, yet it is especially crucial since proper care of MCS patients can lead in some cases to full recovery of consciousness [8].

In clinical practice, the demonstration of self or environmental awareness required for MCS diagnosis – and not for UWS diagnosis – is made through the assessment of a number of reproducible cognitively mediated behaviors, *e.g.* purposeful behaviors, which are clearly distinguishable from reflexive activity. To this end, several assessment scales for post-comatose states have been designed. One of the most popular and widely used one is the JFK Coma Recovery Scale–Revised (CRS-R) [3]. The CRS-R is divided into several assessment subscales (auditory function, motor function, visual function, etc.), and incorporates in its visual function subscale the assessment of visual pursuit, *i.e.* of pursuit eye movement in direct response to a moving stimulus. Indeed, visual pursuit is a strong behavioral marker that, if present, is sufficient to diagnose MCS and discard UWS [2].

In order to create the moving visual stimulus necessary to assess visual pursuit, the CRS-R Administration and Scoring Manual (available from the authors of the CRS-R by request) recommends to clinicians to move a hand mirror in multiple trials right in front of the patient's face so that he/she might follow his/her own reflection. Following this recommendation, the use of this autoreferential stimu-

lus was shown to be consistently more reliable for declaring visual pursuit in MCS patients in comparison with other stimuli, *e.g.* a moving person, with which some MCS patients showed no pursuit at all even though they were actually able to follow a moving mirror [16]. This result was also confirmed in [13], with additional insight being given on the influence of the mirror trajectories chosen during the clinical assessment procedure.

While the research on visual pursuit assessment for MCS diagnosis has provided clinicians with precise and meaningful guidelines, this assessment in practice only relies on subjective categorical estimates made by the clinician about the eye tracking ability of the patient. Indeed, the end result of visual pursuit assessment consists of a "follows" or "does not follow" statement with no further details and based solely on the personal decision of the clinician doing the assessment. These estimates can obviously be biased and impact the overall MCS diagnosis. For such a sensitive task, objective and quantitative measures are desirable as additional information that can be used by the clinician to refine the outcome of the assessment.

In this paper, we present a new, complete system to assist clinicians in the assessment of visual pursuit for MCS diagnosis, which we designed in collaboration with DoC experts. While letting the clinician perform the assessment procedure in the recommended manner, *i.e.* by means of the moving mirror stimulus, our system works alongside using cameras and computer vision techniques to produce a continuous confidence score about the ability of the subject to follow the moving mirror. More specifically, our system tracks the mirror held by the clinician as well as the subject's pupil, then performs a correlation analysis on the obtained trajectories to give an objective measure of the visual pursuit ability. During the whole procedure, no changes are required in the posture and behavior of either the clinician or the patient as compared to visual pursuit assessment performed without the proposed system.

Our system contributes in two very useful ways to the task of visual pursuit assessment for MCS diagnosis. First, it helps clinicians enhance their subjective assessment of visual pursuit by providing an informative and fine-grained objective score relative to this assessment. Second, it does so while preserving the established clinical procedure which was validated as optimal and is widely used in clinical practice. To our knowledge and according to DoC experts, our system is the first to have both of these important characteristics. An earlier study – the closest to our work – used off-the-shelf eye tracking technology and visual stimuli displayed on a computer monitor to quantitatively assess visual pursuit by on- and off-target fixation statistics [14, 15]. In comparison to our system, this earlier system exhibits two weaknesses: (1) it does not – and cannot as it stands – conform to the recommended practice of using
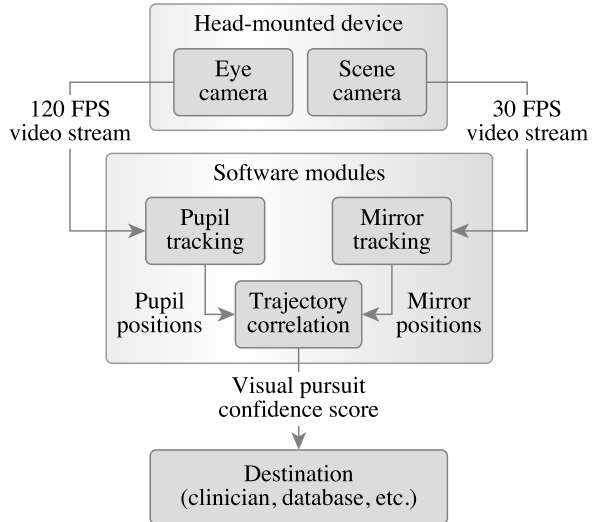

Figure 1. Overview of our system.

a mirror, and uses suboptimal stimuli instead [16, 13]; (2) it necessitates extra subject participation by requiring patients to be seated in order to face the monitor displaying the stimuli, a collaborative behavior which is often unfeasible in clinical practice and necessarily leads to the exclusion of some patients from such assessment.

The rest of this paper is organized as follows. Section 2 describes our system, notably the computer vision techniques used. Section 3 presents the experimental results obtained with our system tested on a set of healthy control subjects, as well as preliminary experimental results with DoC patients. Section 4 concludes.

2. Material and Methods

2.1. System Overview

Figure 1 depicts our complete system. The image acquisition part of the system consists of a lightweight head-mounted device (Fig. 2) with two cameras that we refer to as the eye camera and the scene camera. The eye camera captures close-up grayscale near-infrared frontal images of the eye of interest (left or right, easily adjustable when needed) at 240x160 pixel resolution and 120 frames per second (FPS). We use here infrared illuminator and sensor, and a beam splitter that is placed in front of the eye and is reflective in the infrared and transparent in the visible to not disturb the subject's vision. The scene camera captures grayscale images of the scene as observed by the subject at 752x480 pixel resolution and 30 FPS. It uses an ultra wide angle fish eye lens with a horizontal field of view of 185° in order to cover the normal human field of vision and to ensure that the hand mirror presented by the clinician to the
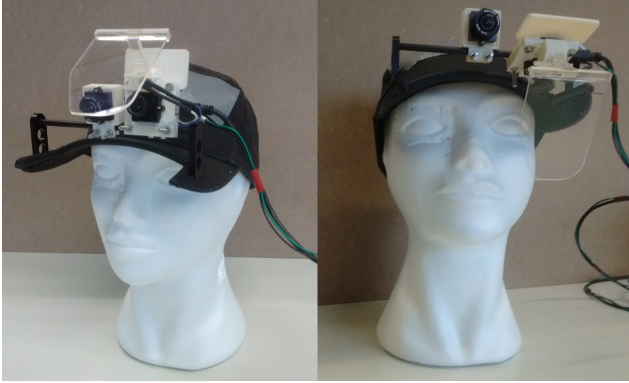
Figure 2. The head-mounted device for the acquisition part of our system. The beam splitter can be raised in order to safely put the device on (left). It is then lowered to enable the capture of close-up frontal images of the eye (right).

subject is also visible by the scene camera.

The eye and scene cameras are connected to a laptop and provide video data to two distinct tracking modules specific to each camera (Fig. 1). One module extracts the 2D position of the pupil in the image reference frame of the eye camera (Sect. 2.2). The other module extracts the 3D position of the hand mirror in the 3D reference frame of the scene camera (Sect. 2.3). A third module filters the synchronized pupil and mirror positions coming from the tracking modules and estimates the correlation between the filtered trajectories (Sect. 2.4). The system outputs a continuous measure of the ability of the subject to follow the hand mirror moved by the clinician; this measure can be interpreted as a confidence score for the presence of visual pursuit. The video data for an assessment session can be recorded on the laptop hard drive. We used this feature to create our experimental evaluation dataset (Sect. 3.3).

2.2. Pupil Detection and Tracking

Video-based eye detection and tracking is a thoroughly studied computer vision problem, due to its many, sometimes challenging applications [4]. In our application, the task is to detect and track the 2D center of the pupil in the images from the eye camera of our system (Sect. 2.1), which removes many difficulties that can occur with other acquisition devices. Indeed, our eye camera is head-mounted and captures in the infrared, which almost completely removes variations in viewpoint and illumination, respectively (inter-subject variations of iris and pupil pixel intensities in particular). It also captures close-up images of the eye alone with a pupil diameter of at least 20 pixels, and the frontal viewpoint makes the pupil appear approximately circular most of the time. The method we propose for pupil detection and tracking is fairly simple because of these advantages offered by our acquisition system.

To detect the pupil center in an image frame I_k, we first remove the few specular reflections by inpainting the very bright areas in I_k, which are detected by adaptive thresholding (using the mean of each pixel's neighborhood), followed by morphological closing. Then, we use a series of synthetic circular concentric iris/pupil templates of varying iris radii and pupil-to-iris ratios to compute a series of correlation images of these templates with I_k. If the largest value of a correlation image does not cross an empirical threshold value, this correlation image is discarded. If all correlation images are discarded, detection is tried again on the next image frame I_{k+1}. If there remains at least one correlation image, we define the coordinates of the pupil center c_k to be the x and y median values of the pixel positions corresponding to the largest values in the remaining correlation images. For further use during tracking, we also define the template T_0 as a circular region of I_k centered at c_k. The radius r_0 of T_0 is set to be the median value of the iris radii in the synthetic templates corresponding to the remaining correlation images.

To robustly track the pupil center in an image frame I_k, we use a template matching approach based on the template update strategy proposed in [9], which was designed to prevent object drift. Namely, we perform two sequential searches within I_k. The first search is made with an updated template T_k, within a small region around the previous pupil center c_{k-1} (extracted from I_{k-1}); the best match of this search gives us the provisional pupil center c_k at frame I_k. The second search is then made within a small region around c_k, with the template T_0 obtained at the time of detection; the best match of this second search gives us c_k^*, a possible drift correction to c_k. The drift correction is applied, i.e. $c_k := c_k^*$, if $||c_k^* - c_k|| \leq \epsilon$, where ϵ is a small empirical threshold. The template T_k is continuously updated during tracking according to the following rule: (1) if $||c_{k-1}^* - c_{k-1}|| \leq \epsilon$, then $T_k := I_{k-1}(c_{k-1}, r_0)$, where the notation $I(c, r)$ denotes the circular region of I centered at c with radius r; (2) if $||c_k^* - c_k|| > \epsilon$, then no update is made to the template.

Blinking or prolonged eye closure causes a temporary absence of the pupil in the image, which may cause the tracking to fail. We tackle this issue by requiring that, during tracking, the best match of the first search (made within the image I_k using the updated template T_k) crosses a empirical threshold value. If not, the tracking is stopped and we perform pupil center detection in subsequent frames to try re-initiating the tracking. Our method for pupil center detection and tracking performs well on our data, as can be seen in Fig. 3.

2.3. Mirror Tracking

In contrast with the problem of tracking the center of the pupil, the problem of tracking a hand-held mirror is not a
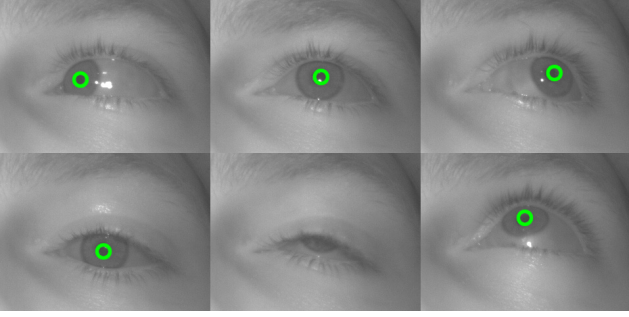
Figure 3. Snapshots of a video taken with the eye camera of our system (Sect. 2.1), with superimposed results obtained with our method for 2D pupil tracking.

customary problem. In fact, we have not found a single paper addressing this issue in detail. We believe that our approach is innovative. Tracking the non-reflective parts of such a mirror, *i.e.* its frame, is similar to the problem of tracking 3D rigid objects in 2D images, which can be solved by calling upon different approaches, *e.g.* fiducial-based tracking, model-based tracking, Interest point-based methods, etc. [7]. However, a hand mirror is mostly a reflective surface, and the reflected patterns in the image indirectly contain information about its 3D pose. Our method for tracking a hand mirror in 3D from 2D images is a model-based tracking method, namely 3D shape model registration by 2D template matching (based on the Lucas-Kanade algorithm [1]), which further incorporates constraints relative to the mirror plane by exploiting the patterns reflected by the mirror.

The 3D shape model $S = \{\mathbf{X}_1, \ldots, \mathbf{X}_n\}$ is a collection of n evenly and densely distributed 3D points lying on the frame surface part that is visible by the camera when the mirror is in a frontal reference pose, with rotation and translation $\{\mathbf{R}_0, \mathbf{t}_0\}$. Our projection model is the perspective camera model, which transforms a 3D point $\mathbf{X}_i = [X_i \ Y_i \ Z_i]^\top$ into its 2D projection $\mathbf{x}_i = [x_i \ y_i]^\top$ in the image plane, via

$$\mathbf{x}_i = \mathbf{K}(\mathbf{R}\mathbf{X}_i + \mathbf{t}), \qquad \mathbf{K} = \begin{bmatrix} f_x & 0 & c_x \\ 0 & f_y & c_y \\ 0 & 0 & 1 \end{bmatrix}, \quad (1)$$

where $\mathbf{R}$ and $\mathbf{t}$ represent the rotation and translation in 3D, respectively, and $\mathbf{K}$ is the calibration matrix with camera intrinsic parameters f_x, f_y (focal lengths in the x and y axes) and c_x, c_y (coordinates of the center of camera), determined via a prior calibration procedure. In our application, the fish eye lens of the scene camera produces strong radial distortion, and calibration must therefore also involve the estimation of the distortion coefficients. Tracking is done on an image with the distortion removed.

The template T is a 2D image of the mirror frame,

also given *a priori*. The relationship between the template T and the shape model S is so that the domain of T is $\{\mathbf{u}_i = \mathbf{K}(\mathbf{R}_0\mathbf{X}_i + \mathbf{t}_0) \ \forall i \in [1 \ldots n]\}$, *i.e.* it corresponds to the projection – with the perspective model in Eq. 1 – of the mirror frame in the reference pose $\{\mathbf{R}_0, \mathbf{t}_0\}$. For ease of explanation here, we present the template T as being constant. In practice it is actually augmented with linear variation allowing for global camera gain and exposure bias.

Using the shape model S, the perspective model and the template T, we can define the first term of the objective function that we will minimize in order to retrieve the mirror pose $\{\mathbf{R}, \mathbf{t}\}$ from an image I. This term is a robust M-estimator of the residuals between the image and the template, given a pose $\{\mathbf{R}, \mathbf{t}\}$:

$$E(I, \mathbf{R}, \mathbf{t}) = \sum_i^n \rho(I(\mathbf{K}(\mathbf{R}\mathbf{X}_i + \mathbf{t})) - T(\mathbf{u}_i)), \quad (2)$$

where ρ is the Huber loss function [1], which down-weights residuals that are likely to come from an occlusion, *e.g.* the hand of the clinician.

To express the constraints about the reflective surface plane, we use a method inspired from [12], where it was shown how the pose of a camera can be estimated provided that the rigid motion between a number of virtual views induced by planar mirror reflections is known. Our case is simplified by the assumption that the mirror pose and, therefore, its plane normal $\mathbf{n}_{k-1}$ and scalar Euclidean distance to the origin d_{k-1} are known *a priori* at frame I_{k-1}. We also make two other assumptions, namely, (1) that the scene camera is fixed, and (2) that the 3D environment being reflected by the mirror is mostly static between two consecutive frames. The differences between the projected reflections in two consecutive frames I_{k-1} and I_k can be thought of as coming from the change of viewpoint of a virtual camera of center $\mathbf{C}_{k-1}^* = 2d_{k-1}\mathbf{n}_{k-1}$, which is symmetric to the real camera of center $\mathbf{C} = \mathbf{0}$ with respect to the moving mirror plane. To retrieve the corresponding virtual camera rotation $\mathbf{R}_k^*$ and translation $\mathbf{t}_k^*$, we use the essential matrix method [5], which exploits the known calibration matrix $\mathbf{K}$ and an estimated fundamental matrix $\mathbf{F}_k$ embodying the epipolar geometry that explains the image correspondences between the projected reflections in frames I_{k-1} and I_k. From the new virtual camera center, obtained by $\mathbf{C}_k^* = \mathbf{R}_k^*\mathbf{C}_{k-1}^* + \mathbf{t}_k^*$, the estimation of the new mirror plane normal is $\mathbf{n}_k = \mathbf{C}_k^* / ||\mathbf{C}_k^*||$, with Euclidean distance to the origin $d_k = -\langle \mathbf{n}_k, \mathbf{C}_k^* / 2 \rangle$. Incorporating a regularizing term that penalizes the distance of the 3D points of the shape model S to this plane, the complete minimization problem for finding the mirror pose $\{\mathbf{R}_k, \mathbf{t}_k\}$ at frame I_k is therefore

$$\underset{\mathbf{R}, \mathbf{t}}{\text{argmin}} \ E(I_k, \mathbf{R}, \mathbf{t}) + C \sum_i^n (\langle \mathbf{R}\mathbf{X}_i + \mathbf{t}, \mathbf{n}_k \rangle + d_k)^2, \quad (3)$$
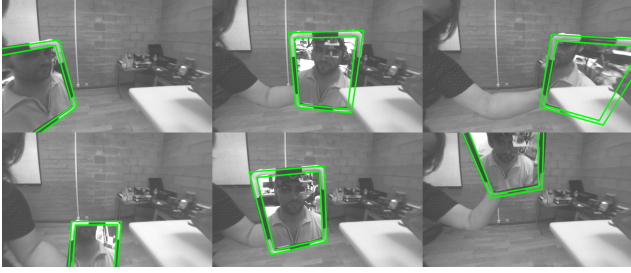
Figure 4. Snapshots of a video taken with the scene camera of our system (Sect. 2.1), with superimposed results obtained with our method for 3D planar mirror tracking.

where $E(I_k, \mathbf{R}, \mathbf{t})$ comes from Eq. 2, and C is an empirical constant multiplier balancing the soft constraint. After a coarse initialization of the mirror pose at the beginning of a scene video, the Gauss-Newton algorithm derived from the optimization problem in Eq. 3 continuously extracts the 3D pose of the mirror robustly in the presence of extreme projective deformation, clutter, and occlusions. Figure 4 illustrates the effectiveness of our approach.

2.4. Trajectory Correlation

The continuous extractions of the 2D image positions of the pupil and the (X, Y) spatial positions of the mirror lead to two trajectories, which are similar in the presence of visual pursuit. Because the tracking modules were designed to be robust, they do not output strong outliers, and we can efficiently remove statistical noise and inaccuracies using Kalman filtering [17]. The two trajectories are defined in reference frames that share the same orientation – the eye and scene cameras are aligned with each other – but have different origins and scales in the horizontal and vertical directions. We can therefore expect the relationship between the 2D pupil and mirror positions to be linear in case of visual pursuit. We use the sample Pearson correlation coefficient [10] to quantify this linearity. We found empirically that it is better to quantify the linearity separately in each of the horizontal and vertical directions and then to average the results. We also ignore results with negative correlations if any. Denoting by $\widehat{x}$ and $\widehat{y}$ the samples of the filtered x and y image positions of the pupil, and by $\widehat{X}$ and $\widehat{Y}$ the samples of the filtered X and Y spatial positions of the mirror, and by r_{ab} the Pearson correlation coefficient between two samples a and b, the confidence score is calculated as follows:

$$\frac{\max(r_{\widehat{x}\widehat{X}},\ 0) + \max(r_{\widehat{y}\widehat{Y}},\ 0)}{2}. \tag{4}$$

Its values are in $[0, 1]$. As an example, Fig. 5 shows the evolution of the confidence score as the pupil and mirror trajectories are extracted over a positive visual pursuit test.

3. Experimental Evaluation

3.1. Subjects

For the experimental evaluation of our system, we enrolled 23 control subjects and five chronic DoC patients. The control subjects were healthy volunteers between the age of 23 and 48 years, 13 of which were male. None of those control subjects was ever diagnosed with visual impairment or consciousness disorder. The patients were enrolled with the consent of their families. Two of these patients were diagnosed with UWS and three with MCS, according to the CRS-R and other standard diagnostic criteria [2, 6]. In particular, results of CRS-R evaluations made before our experiments showed that the three MCS patients considered here were able to perform visual pursuit (according to the criteria described in Sect. 3.2).

3.2. Clinical Procedure

In all our experiments, the visual pursuit assessment procedure was performed by a skilled clinician who used the moving mirror stimulus according to the CRS-R protocol, as described next. First, the clinician holds a hand mirror at about 15 centimeters right in front of the subject's face and verbally encourages the subject to fixate the mirror (this last point was subject to modifications in some experiments, see Sect. 3.3). Then, the clinician moves the mirror slowly at 45 degrees to the right and left of the vertical midline of the subject's face, and 45 degrees above and below his/her horizontal midline. This must be done while keeping the mirror at a constant distance from the subject's face and ensuring that the subject might follow his/her own reflection. The exact order of these four movements is to be chosen by the clinician; in our experiments, the clinician aimed at making them as random as possible in order to avoid evaluation bias. The above series of four movements is then repeated so that a total of eight visual pursuit trials, two in each direction, are performed. The presence of visual pursuit is declared by the clinician if the subject follows the mirror for 45 degrees without loss of fixation, on at least two occasions in any direction.

3.3. Experiments

The experiments with the control subjects were all conducted in the same laboratory environment, while the experiments with the patients were conducted in their respective rooms in a hospital environment. The control subjects were seated casually, while the patients could lie in bed in their favorite, most comfortable position. For the control subjects as well as for the patients, the head-mounted device (Sect 2.1) was placed by the clinician on the subject prior to the actual visual pursuit assessment procedure. The laptop connected to the eye and scene cameras of the head-mounted device was placed on a table nearby, out of view

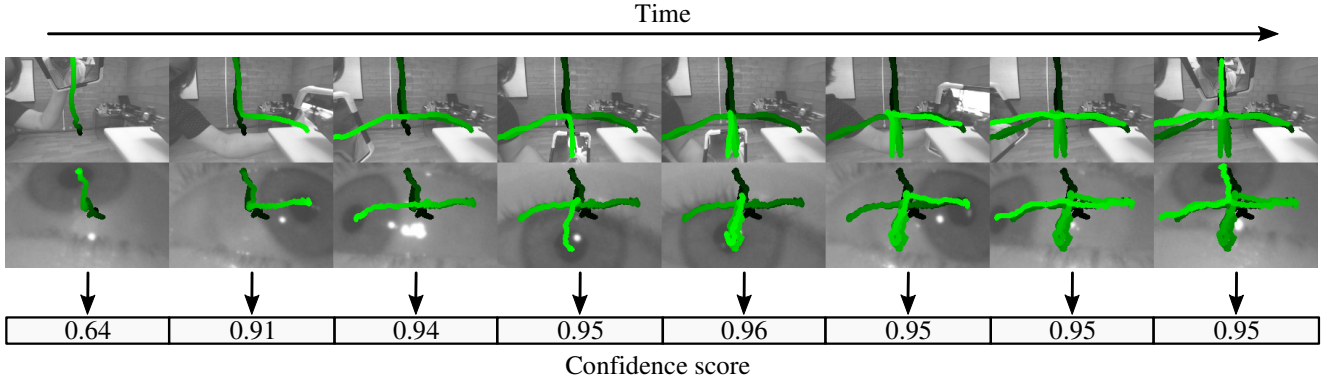| 0.64 | 0.91 | 0.94 | 0.95 | 0.96 | 0.95 | 0.95 | 0.95 |

Confidence score

Figure 5. Time-lapse image sequence of a visual pursuit test with a positive outcome, illustrating the production of the pupil and mirror trajectories, along with the derived confidence score. The trajectories are drawn in fading green to visualize the progress in time (the brighter the green is, the more recently the trajectory point was extracted). The pupil and mirror trajectories look similar because of the presence of visual pursuit; this is corroborated by the evolution of the confidence score which quickly reaches a value close to 1.

of the subject being tested. These preparatory steps are very simple and performed within a few seconds.

After the preparatory steps were made for a subject (either control or patient) the clinician performed the visual pursuit assessment procedure as described in Sect. 3.2, while our system simultaneously recorded the eye and scene videos corresponding to this assessment. These videos were later processed off-line to output a confidence score for the presence of visual pursuit in the tested subject (Sect. 2). These experimental sessions were performed once for each of the 23 control subjects and each of the five patients.

In order to test the sensitivity of our system to the eye behavior, we conducted additional experiments with the control subjects. For 17 of them, we organized another session where they were verbally encouraged by the clinician to focus their gaze on a fixed point and not to try following the moving mirror. Also, for 10 of the control subjects, we organized another session where they were verbally encouraged to perform random eye movements and to ignore as best as possible the moving mirror. The general experimental setup remained unchanged for these additional experiments.

Our experimental data is therefore divided into four groups of subjects: 23 control subjects who were encouraged to follow the moving mirror (CS1), 17 control subjects who were encouraged to keep a fixed gaze (CS2), 10 control subjects who were encouraged to do random eye movements (CS3), and five DoC patients who were encouraged to follow the moving mirror (DoC), including three MCS and two UWS.

3.4. Results

Figure 6a presents, as box plots, the distributions of the confidence score obtained with our system for the groups of control subjects (Sect. 3.3). For the CS1 group, instructed

to follow the mirror, the median score is 0.92, the maximum score is 0.96, and the minimum score is 0.79, which is the only outlier of the group. For the CS2 group, instructed to keep a fixed gaze, the median score is 0.01, the minimum score is 0.0, and the maximum score is 0.25, which is the only outlier of the group. For the CS3 group, instructed to perform random eye movements, the median and minimum scores are both 0.0 and the maximum score is 0.31, which is the only outlier of the group. Overall, the confidence scores for the control subject groups are as expected, according to the instructions given by the clinician, *i.e.* close to the maximal value of 1.0 for CS1 and close to the minimal value of 0.0 for CS2 and CS3. After visual inspection of the videos corresponding to the outliers in groups CS2 and CS3, we observed that those subjects had difficulties to ignore the moving mirror, showing brief, self-restrained intentions to follow it. On the other hand, the outlier subject in group CS1 performed a visual pursuit with pronounced saccadic eye movements, for an unknown reason.

Figure 7 shows the time evolution, over the visual pursuit assessment procedure, of the average confidence score for each of the three groups of control subjects CS1, CS2 and CS3. This figure shows that the confidence score quickly discriminates between pursuit and no pursuit in the experiments designed with the healthy subjects. Indeed, the average score reaches above 0.9 for the CS1 group who was instructed to follow the mirror, and below 0.1 for the CS2 and CS3 groups when barely half of the total assessment procedure has been performed.

Figure 6b shows the preliminary results obtained with our system for the group of DoC patients. The two UWS patients had a score of 0.03 and 0.07, respectively, and the clinician confirmed that those patients showed no presence of visual pursuit. The three MCS patients had a score of 0.41, 0.49, and 0.7, respectively, and the clinician declared
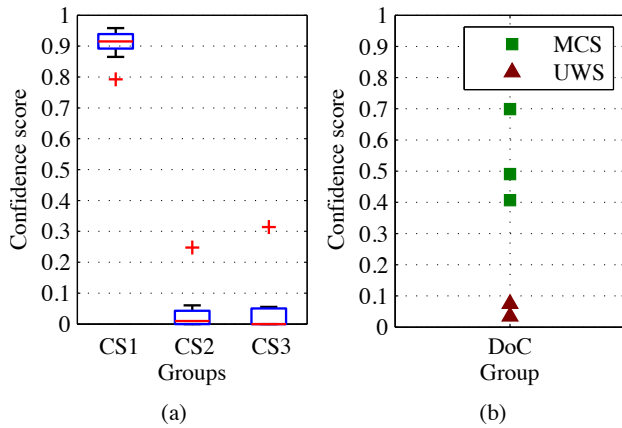
Figure 6. Confidence scores obtained with our system. (a) Box plots of the score distributions for the control subject groups. (b) Scores obtained for the group of five DoC patients.
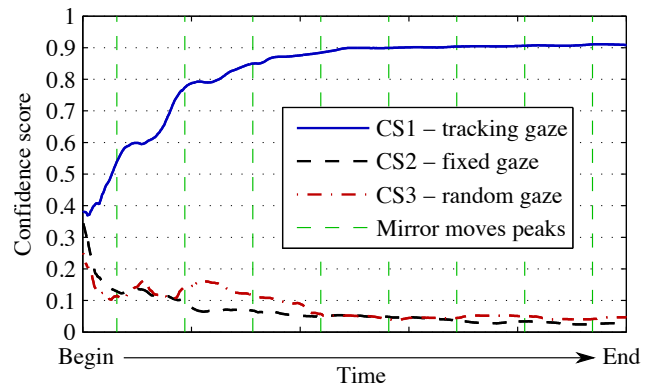

Figure 7. Time evolution, over the assessment procedure, of the confidence scores in the control subject groups. The eight green vertical dashed lines correspond to the approximate moments when the clinician reaches the peak of a trial mirror movement.

visual pursuit for the three of them. Interestingly, before being communicated our system's result for the MCS patient with a score of 0.41, the clinician commented that she had first been hesitant to declare visual pursuit for this patient. This confirms the usefulness of a system such as the one we propose here. Indeed, a confidence score of 0.41 with our system allows the clinician to clear the doubts associated with a purely subjective assessment.

4. Conclusions

Accurate diagnosis of MCS is a challenging, yet crucial task, as MCS patients might recover consciousness provided they are given appropriate clinical management. Because the subtle behavioral markers subjectively assessed in clinical practice are inevitably subject to experimental bias, clinicians and researchers working in the field of disorders of consciousness, and eventually patients, can greatly benefit from objective assisting systems. We believe that the new system presented in this work is a step forward in that direction. Using cameras and computer vision techniques, it provides an objective score of confidence for the presence of the important marker that is visual pursuit, as additional insight for the clinician who can use it to enhance his/her own assessment. Furthermore, it does so while conforming to the recommended and validated practice of using a hand mirror to create the moving visual stimulus. Through experimental results with healthy control subjects, we showed that our system is accurate and reliable in a laboratory environment. The preliminary experimental results with UWS and MCS patients suggest that our system can be used in a hospital environment with benefits. In future work, we plan to provide a clinical validation of our system by testing it with a large group of MCS patients.

References

[1] S. Baker and I. Matthews. Lucas-kanade 20 years on: A unifying framework. *Int. J. Comput. Vision*, 56(3):221–255, 2004.

[2] J. T. Giacino, S. Ashwal, N. Childs, et al. The minimally conscious state definition and diagnostic criteria. *Neurology*, 58(3):349–353, 2002.

[3] J. T. Giacino, K. Kalmar, and J. Whyte. The JFK Coma Recovery Scale-Revised: measurement characteristics and diagnostic utility. *Arch. Phys. Med. Rehabil.*, 85(12):2020–2029, 2004.

[4] D. W. Hansen and Q. Ji. In the eye of the beholder: a survey of models for eyes and gaze. *IEEE Trans. Pattern Anal. Mach. Intell.*, 32(3):478–500, 2010.

[5] R. Hartley and A. Zisserman. *Multiple view geometry in computer vision*. Cambridge University Press, 2003.

[6] S. Laureys, G. G. Celesia, F. Cohadon, et al. Unresponsive wakefulness syndrome: a new name for the vegetative state or apallic syndrome. *BMC Med.*, 8(1):68, 2010.

[7] V. Lepetit and P. Fua. *Monocular model-based 3D tracking of rigid objects*. Now Publishers Inc, 2005.

[8] J. Luaute, D. Maucort-Boulch, L. Tell, et al. Long-term outcomes of chronic minimally conscious and vegetative states. *Neurology*, 75(3):246–252, 2010.

[9] I. Matthews, T. Ishikawa, and S. Baker. The template update problem. *IEEE Trans. Pattern Anal. Mach. Intell.*, 26(6):810–815, 2004.

[10] A. J. Onwuegbuzie, L. Daniel, and N. L. Leech. Pearson product-moment correlation coefficient. In N. J. Salkind, editor, *Encyclopedia of measurement and statistics*, pages 751–756. SAGE Publications, Inc., 2007.

[11] F. Plum and J. B. Posner. *The diagnosis of stupor and coma*. Contemp. Neurol. Ser. F.A. Davis Company, 1966.

[12] R. Rodrigues, J. P. Barreto, and U. Nunes. Camera pose estimation using images of planar mirror reflections. In *Proc. ECCV'10*, volume 4, pages 382–395, 2010.

[13] M. Thonnard, S. Wannez, S. Keen, et al. Detection of visual pursuit in patients in minimally conscious state: a matter of stimuli and visual plane? *Brain Inj.*, 28(9):1164–1170, 2014.

[14] L. Trojano, P. Moretta, V. Loreto, et al. Quantitative assessment of visual behavior in disorders of consciousness. *J. Neurol.*, 259(9):1888–1895, 2012.

[15] L. Trojano, P. Moretta, V. Loreto, et al. Affective saliency modifies visual tracking behavior in disorders of consciousness: a quantitative analysis. *J. Neurol.*, 260(1):306–308, 2013.

[16] A. Vanhaudenhuyse, C. Schnakers, S. Brédart, and S. Laureys. Assessment of visual pursuit in post-comatose states: use a mirror. *J. Neurol. Neurosurg. Psychiatry*, 79(2):223, 2008.

[17] G. Welch and G. Bishop. An introduction to the Kalman filter. Technical report, University of North Carolina at Chapel Hill, 1995.